Supplementary Information

Anion-mediated approach to overcome oxidation in ether electrolytes for high-voltage sodium-ion batteries

Xingyu Wang[1]†, Qi Fan[1]†, Ziheng Liu[1]†, Xinyue Zhu[2], Mei Yang[1], Zhiyuan Guo[1], Yuting Chen[1], Liuqi Wang[1], Yu Jing[2]* & Hui Xia[1]**

[1]School of Materials Science and Engineering, Nanjing University of Science and Technology, Nanjing 210094, China

E-mail: bayberry616@163.com (M. Y.); xiahui@njust.edu.cn (H. X.)

[2]Jiangsu Co-Innovation Centre of Efficient Processing and Utilization of Forest Resources, College of Chemical Engineering, Nanjing Forestry University, Nanjing 210037, China

E-mail: yujing@njfu.edu.cn (Y. J.)

Keywords: (sodium-ion batteries, cathode-electrolyte interface (CEI), solvation structure, ether electrolyte, high voltage)

Supplementary Figures

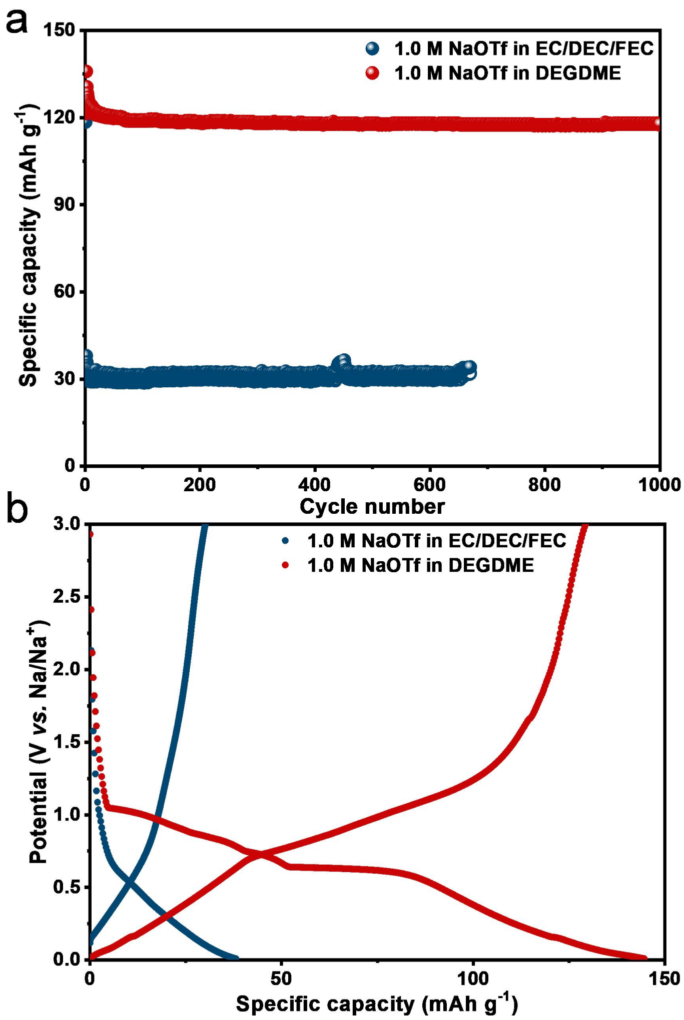

Supplementary Fig. 1 Electrochemical performance of graphite negative materials. (a) Cycling capabilities and (b) GCD curves in carbonate and G2 electrolytes.

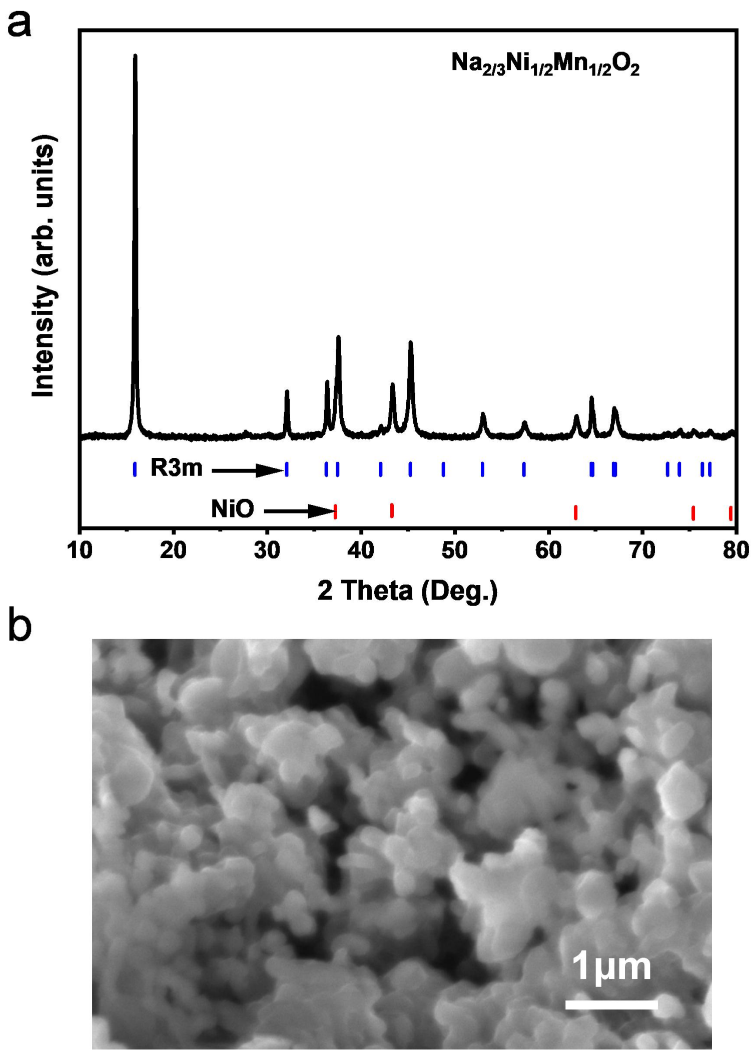

Supplementary Fig. 2 Materials characterization of $Na_{2/3}Ni_{1/2}Mn_{1/2}O_2$ (NNM) particles. (a) XRD pattern and (b) SEM image.

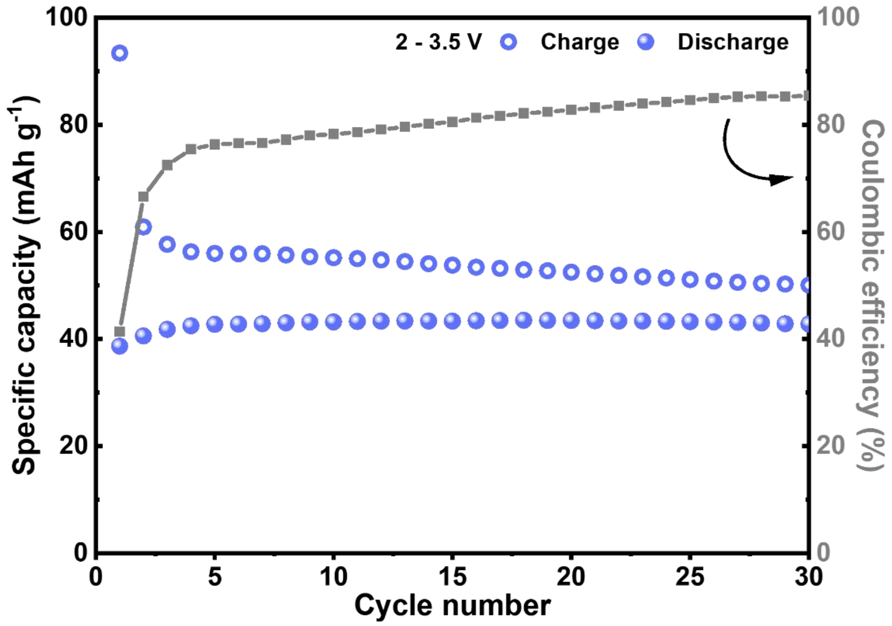

Supplementary Fig. 3 Cycling capability of Na||NNM half-cell in G2 electrolyte, within a cut-off voltage of 3.5 V.

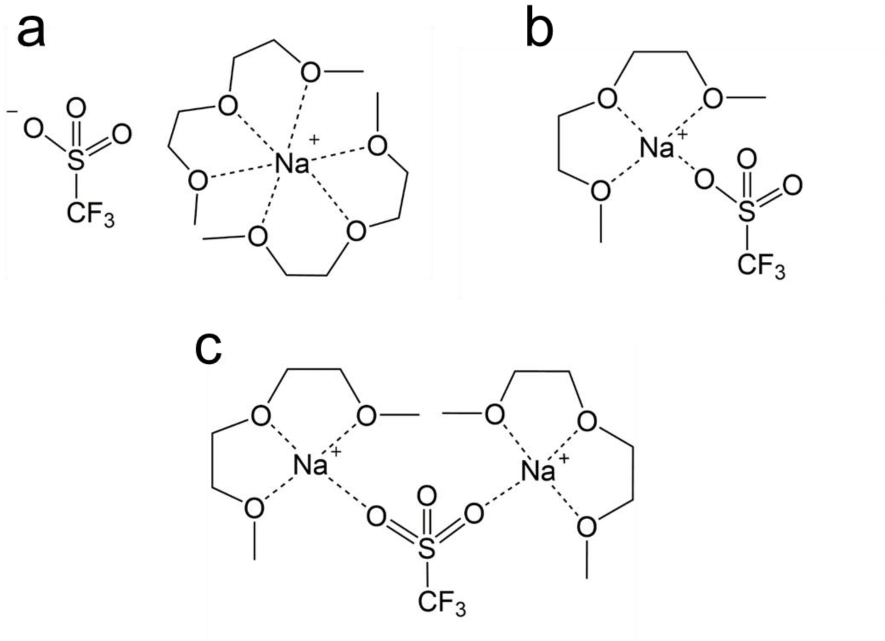

Supplementary Fig. 4 Possible solvation structures in G2 electrolyte. (a) FI, (b) CIP and (c) AIP.

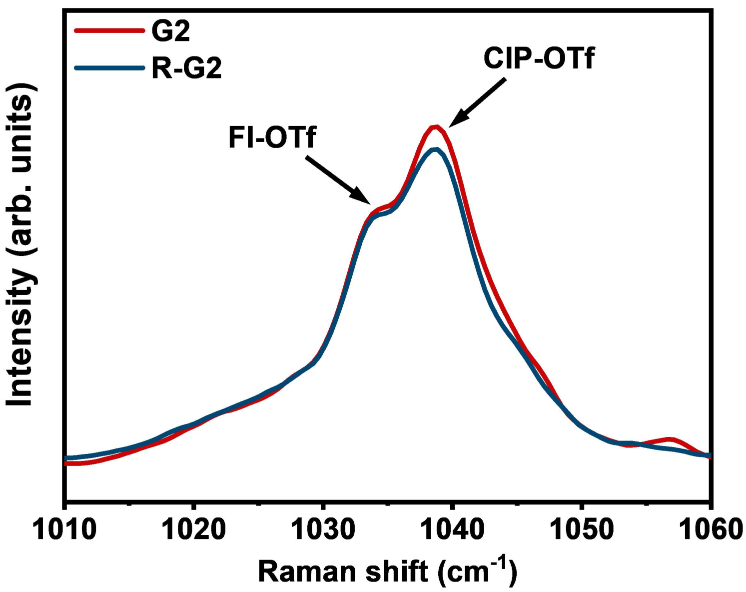

Supplementary Fig. 5 Raman spectra of G2 and R-G2 electrolytes between 1010 to 1060 cm^{-1}.

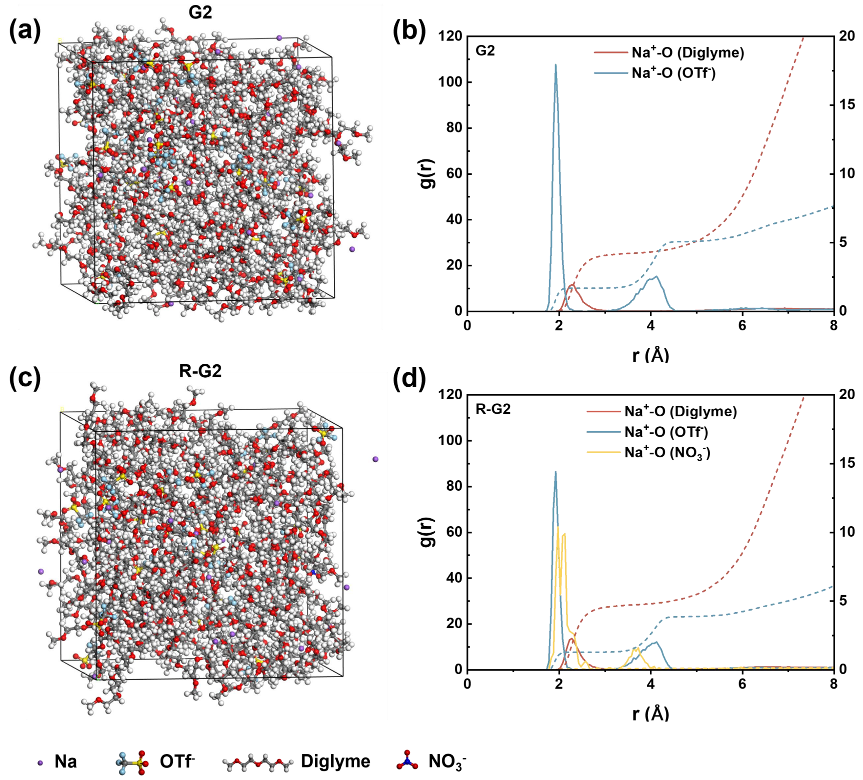

Supplementary Fig. 6 MD analysis of electrolyte environment. Snapshots of simulated (a) G2 electrolyte and (c) R-G2 electrolyte, together with (b) and (d) corresponding RDF distributions.

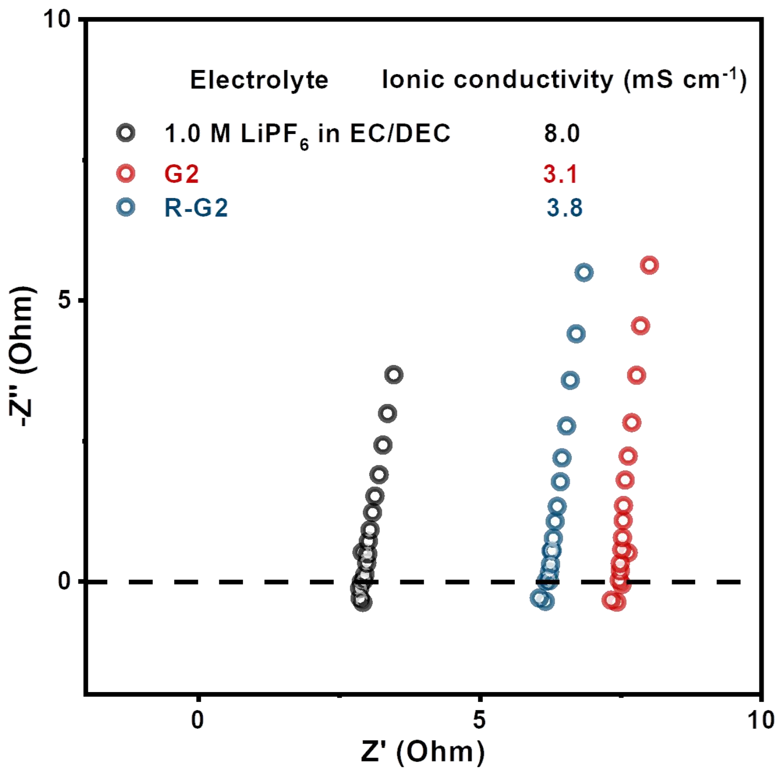

Supplementary Fig. 7 Ionic conductivity of 1.0 M $LiPF_6$ in ethylene carbonate (EC)/diethyl carbonate (DEC), 1.0 M $NaPF_6$ in G2 and 1.0 M $NaPF_6$ in R-G2 electrolyte. 1.0 M $LiPF_6$ in EC/DEC is used as reference.

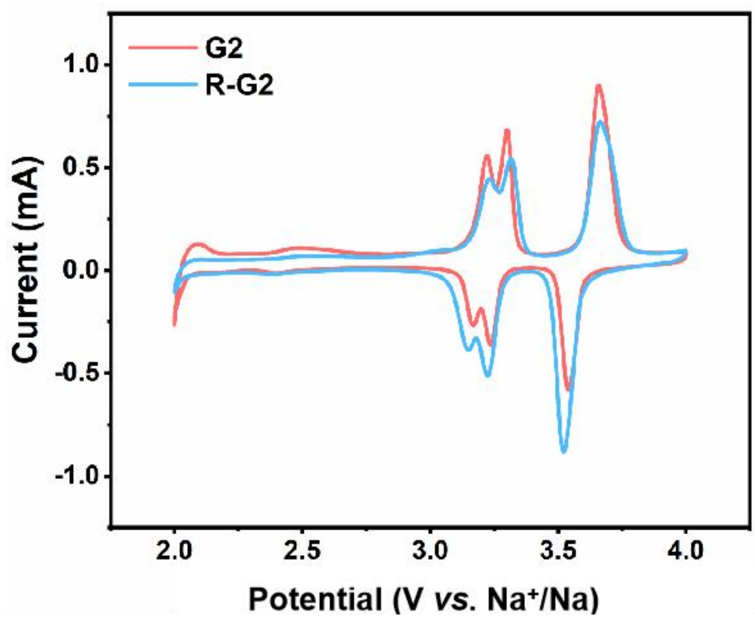

Supplementary Fig. 8 CV curves of Na||NNM cells for the second cycle with G2 and R-G2 electrolytes.

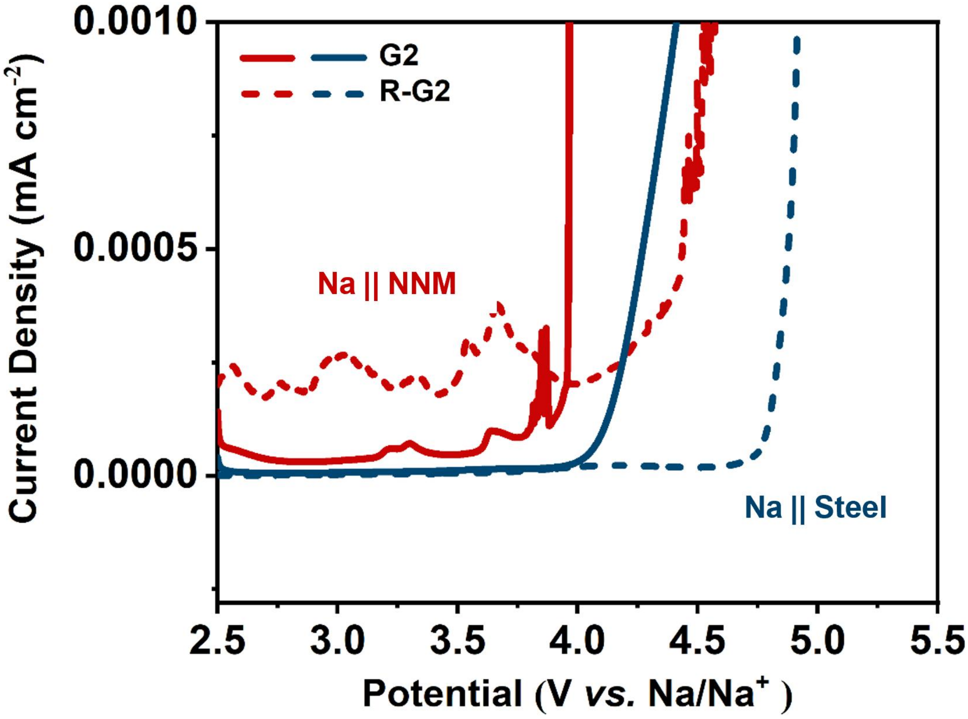

Supplementary Fig. 9 Enlarged detail from the LSV curves of Figure 3a, highlighting the current peak associated with Na^+ intercalation in Na||NNM cells.

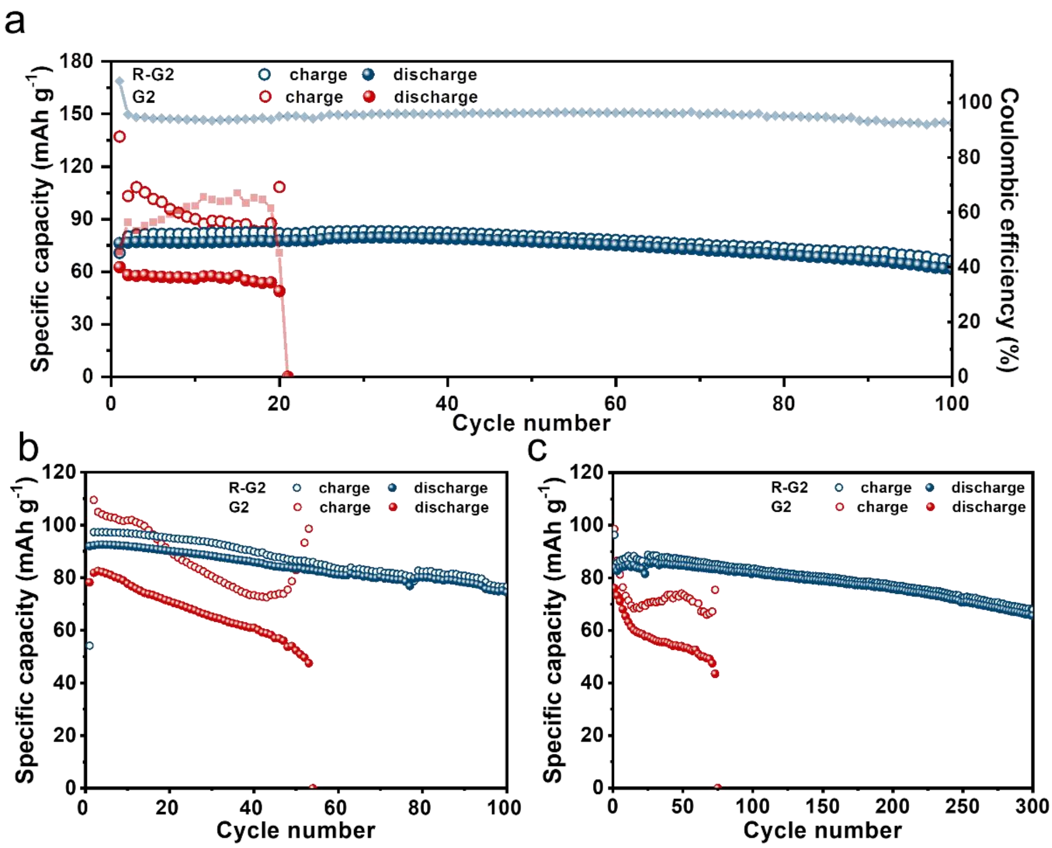

Supplementary Fig. 10 Electrochemical performance of half-cells in G2 and R-G2 electrolytes. Cycling capability of half-cells with (**a**) NNM, (**b**) tunnel NMO and (**c**) NVP positive electrode materials.

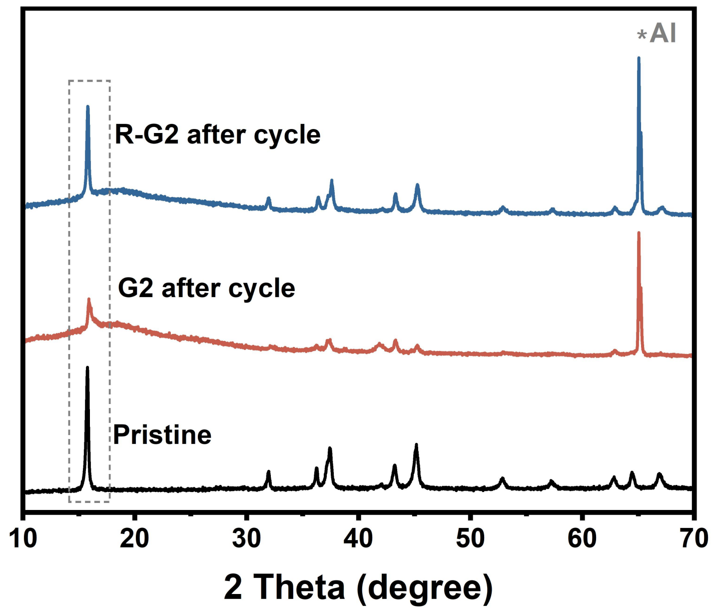

Supplementary Fig. 11 XRD patterns of the NNM electrodes after 5 cycles with G2 and R-G2 electrolytes.

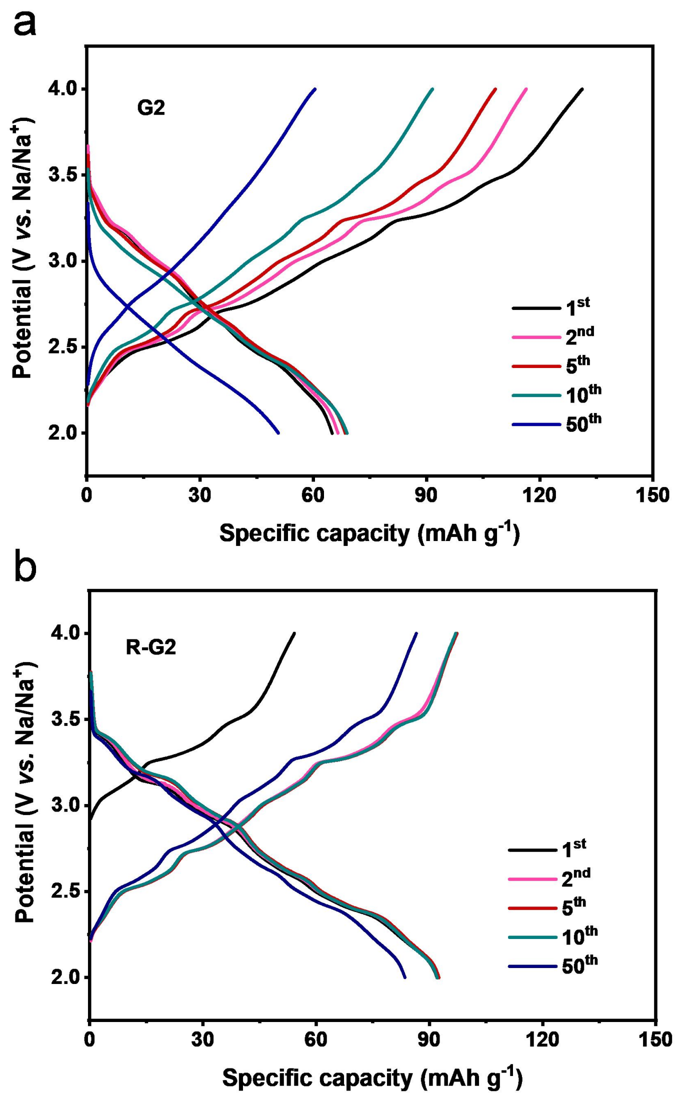

Supplementary Fig. 12 GCD profiles comparison of tunnel Na||NMO cells. GCD profiles in (a) G2 and (b) R-G2 electrolytes with a voltage window of 2.0-4.0 V vs. Na/Na^+.

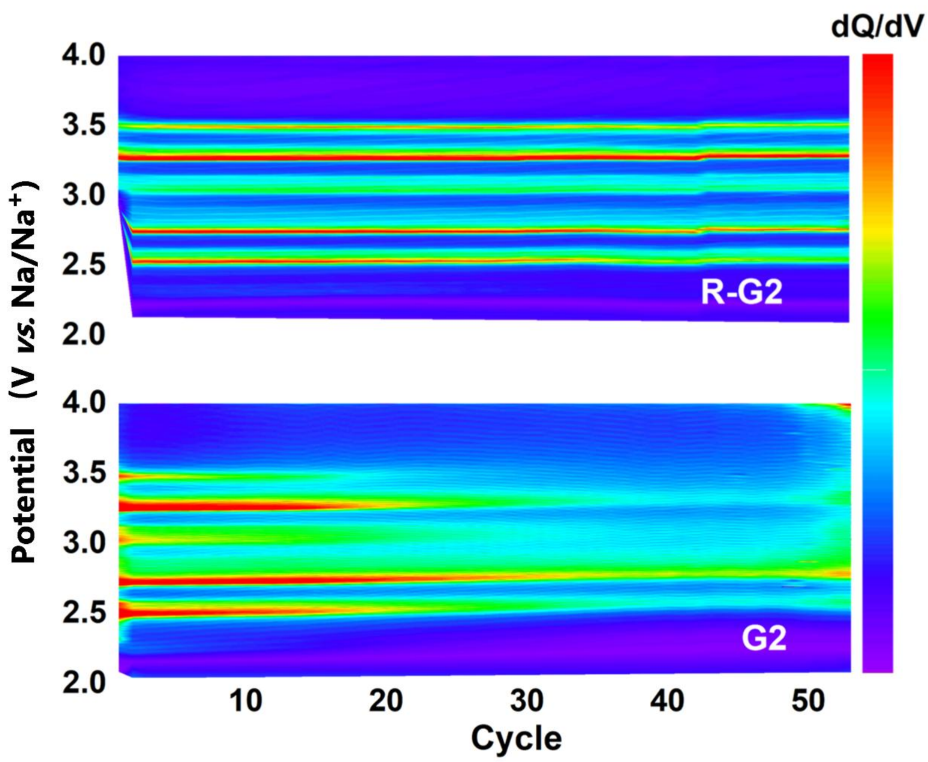

Supplementary Fig. 13 The dQ/dV contour map of of tunnel Na||NMO cells in G2 and R-G2 electrolytes.

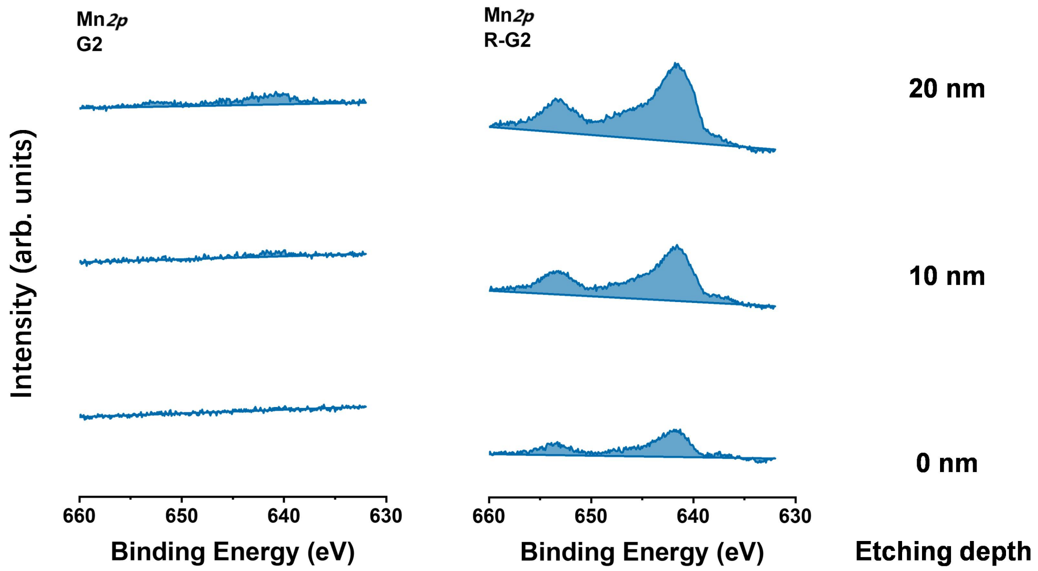

Supplementary Fig. 14 Mn *2p* XPS spectra of the NNM electrodes cycled with G2 and R-G2 electrolytes.

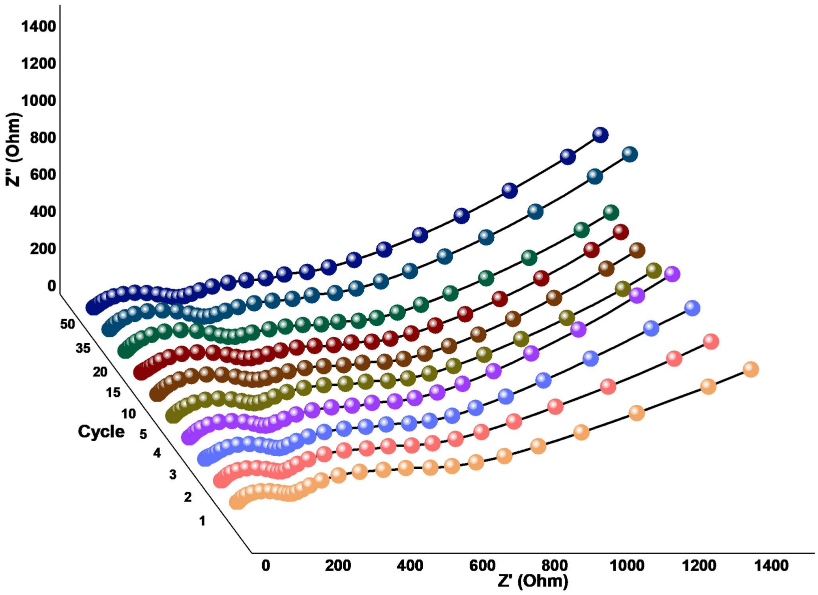

Supplementary Fig. 15 EIS spectrum of different cycles in R-G2 electrolyte with NNM cathode.

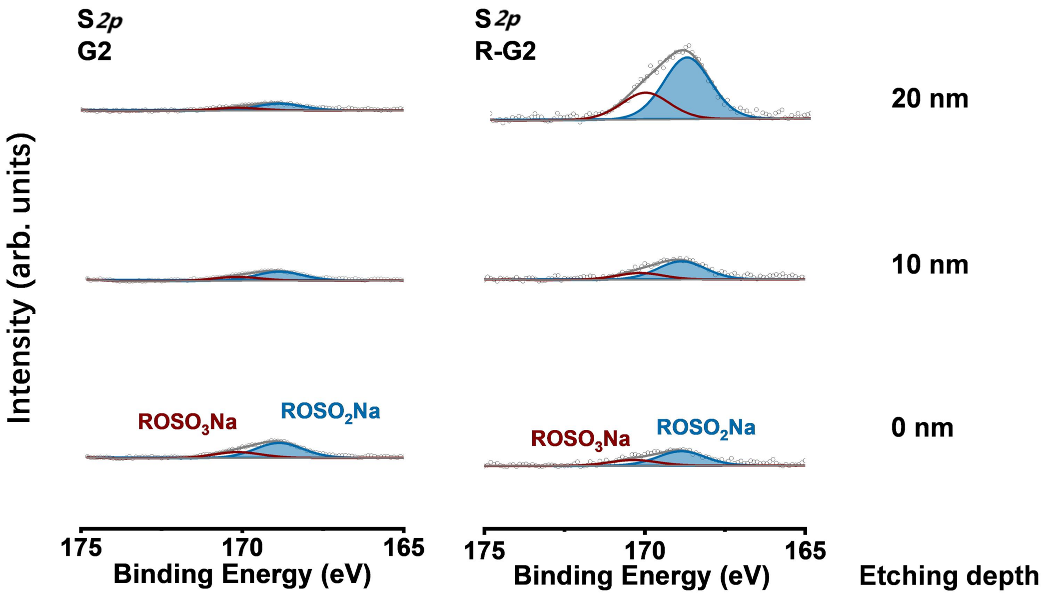

Supplementary Fig. 16 S *2p* XPS spectra of the NNM electrodes cycled with G2 and R-G2 electrolytes.

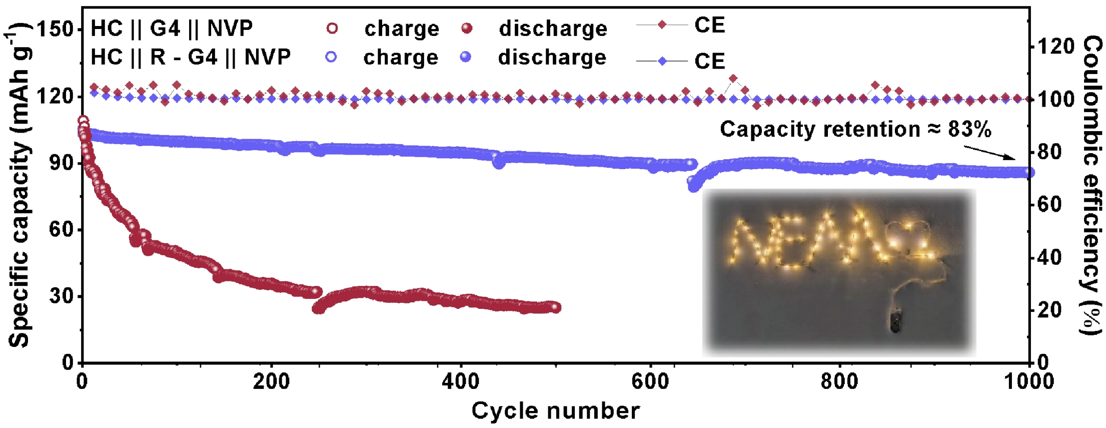

Supplementary Fig. 17 Cycling capability of HC||NVP full cells in G4 and R-G4 electrolytes at 100 mA g^{-1}. Inset shows the lighting demonstration of a full cell.

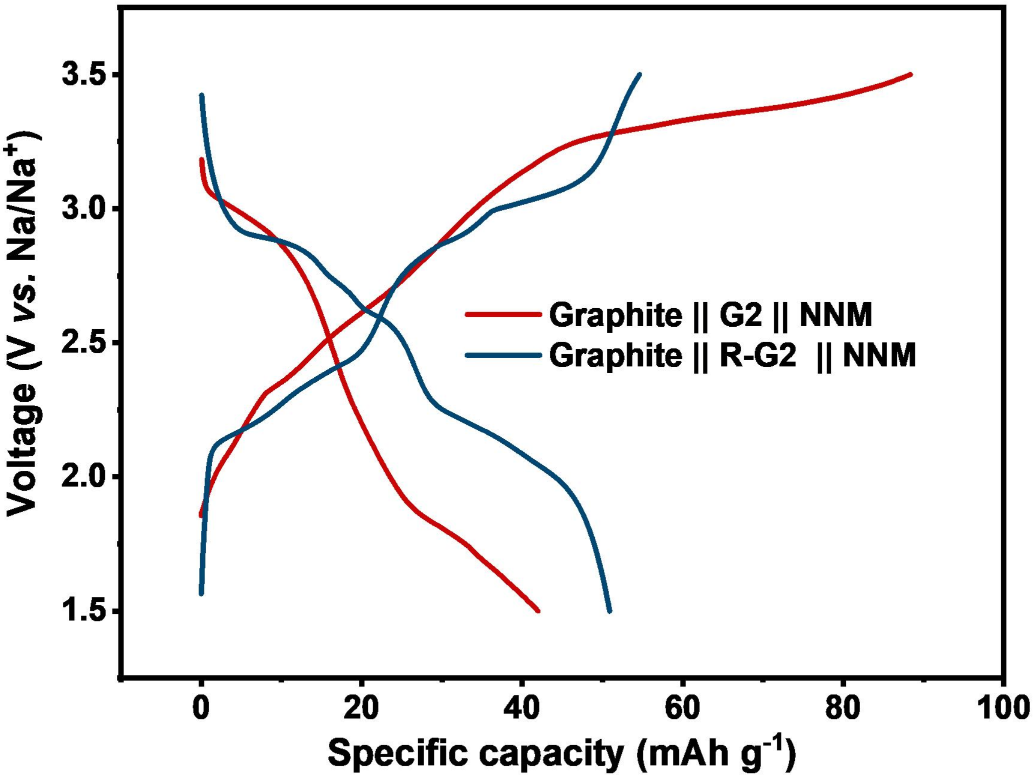

Supplementary Fig. 18 Typical GCD profiles of graphite||NNM full batteries.

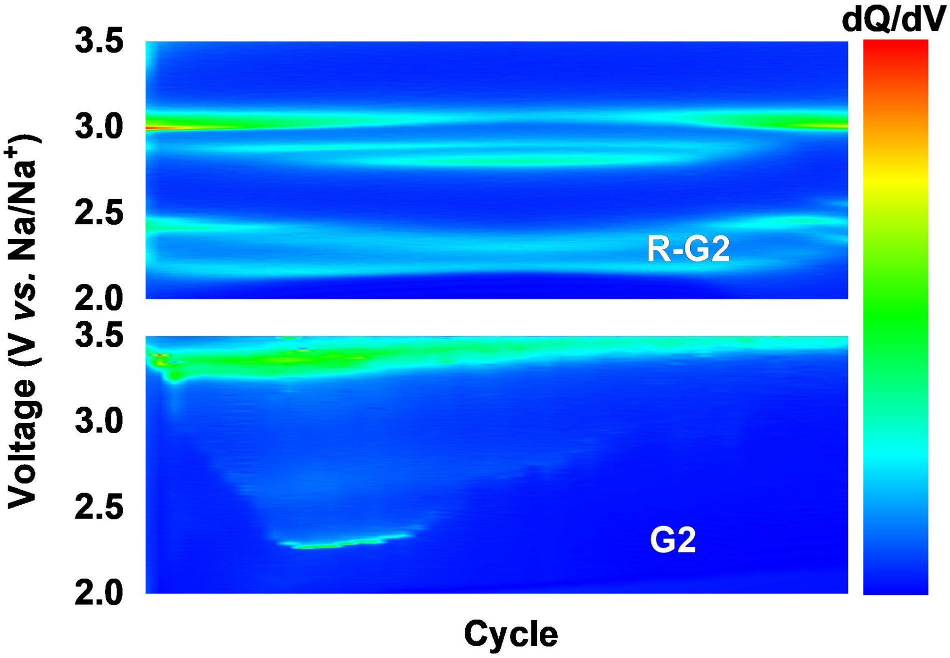

Supplementary Fig. 19 The dQ/dV contour map of graphite||NNM full batteries with a voltage window of 2-3.5 V vs Na/Na^+.

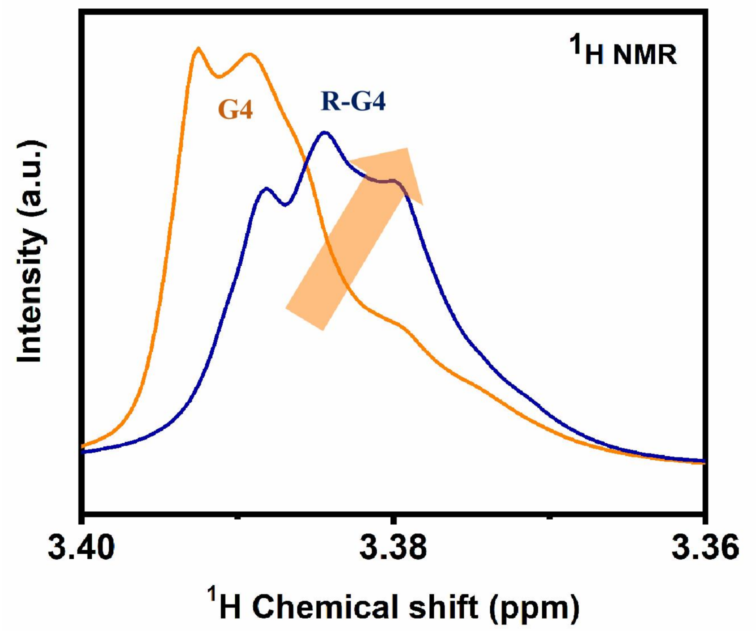

Supplementary Fig. 20 ^{1}H NMR comparison of G4 and R-G4 electrolytes.

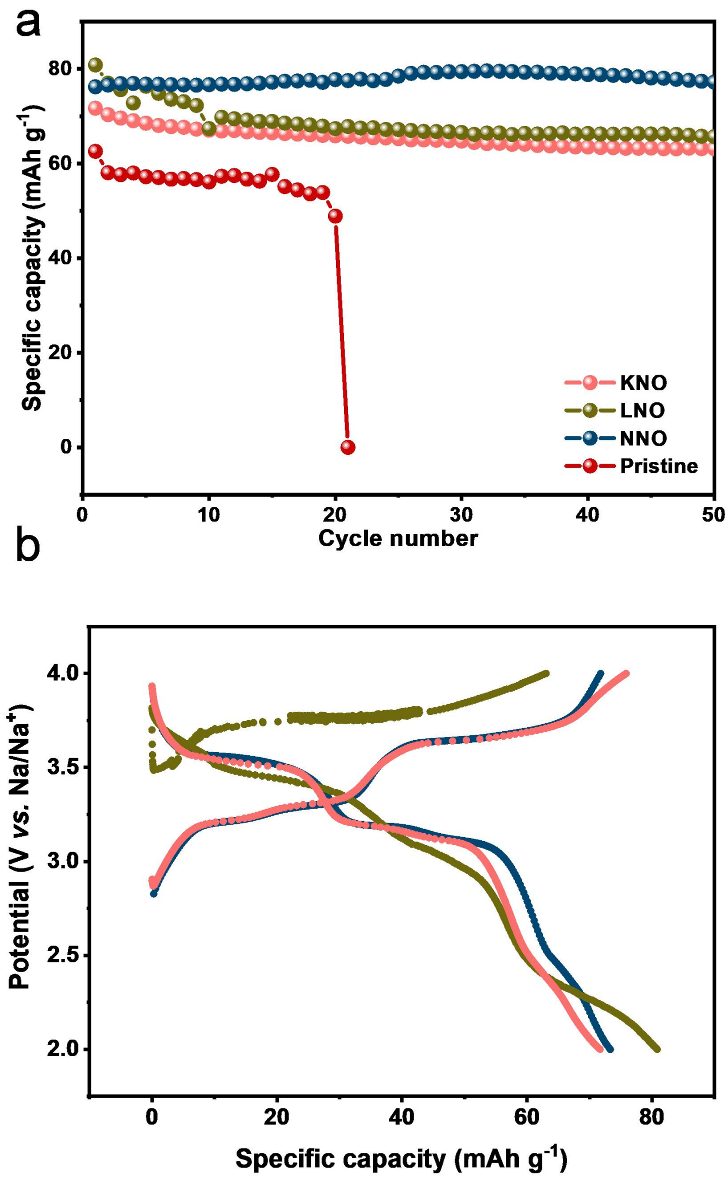

Supplementary Fig. 21 Electrochemical performance with $LiNO_3$, $NaNO_3$ and KNO_3 additives in G2 electrolyte (denoted as LNO, NNO and KNO, respectively). (a) Cycling capabilities and (b) GCD curves of NNM positive electrodes with saturated LNO, NNO and KNO, respectively.

Supplementary Tables

Supplementary Table 1 | Electrochemical performance of some typical SIB anode materials in G2 electrolyte.

Material	Voltage vs. Na^+/Na (V)	Initial Coulombic efficiency	Cycle (current density, A g^{-1}) (capacity retention)	Capacity (mAh g^{-1}) (Current density, A g^{-1})	Ref.
FeS_2 nanoclusters	0.01 - 3	92 %	10000 (10) (92.7%)	749.6 (0.1)	1
Hard carbon paper	0.01 - 2	91.2 %	1000 (0.2) (93%)	338.2 (0.02)	2
VS_2 nanosheets	0.3 - 3	94 %	700 (5) (87%)	600 (0.1)	3
Co_4S_3 nanosheets	0.5 - 3	86 %	400 (1) (80%)	571 (0.1)	4
Graphite	0.01- 2	91 %	6000 (0.2) (95%)	110 (0.1)	5

Supplementary References

1. Wan, Y. H. et al. Ultra-high initial coulombic efficiency induced by interface engineering enables rapid, stable sodium storage. *Angew. Chem.-Int. Ed.* **60**, 11481-11486 (2021).

2. Hou, B. H. et al. Self-supporting, flexible, additive-free, and scalable hard carbon paper self-interwoven by 1D microbelts: superb room/low-temperature sodium storage and working mechanism. *Adv. Mater.* **31**, 1903125 (2019).

3. Yu, D. X. et al. Hierarchical flower-like VS_2 nanosheets - a high rate-capacity and stable anode material for sodium-ion battery. *Energy Storage Mater.* **11**, 1-7 (2017).

4. Dong, Y. F. et al. 2D holey cobalt sulfide nanosheets derived from metal-organic frameworks for high-rate sodium ion batteries with superior cyclability. *J. Mater. Chem. A.* **6** , 14324-14329 (2018).

5. Zhu, Z. Q., Cheng, F. Y., Hu, Z., Niu, Z. Q. & Chen, J. Highly stable and ultrafast electrode reaction of graphite for sodium ion batteries. *J. Power Sources.* **293**, 626-634(2015).